Polymodal activation of the TREK-2 K2P channel produces structurally distinct open states

Conor McClenaghan,[1,2] Marcus Schewe,[4] Prafulla Aryal,[1,2] Elisabeth P. Carpenter,[2,3] Thomas Baukrowitz,[4] and Stephen J. Tucker[1,2]

[1]Clarendon Laboratory, Department of Physics and [2]OXION Initiative in Ion Channels and Disease, University of Oxford, Oxford OX1 3PU, England, UK
[3]Structural Genomics Consortium, University of Oxford, Oxford OX3 7DQ, England, UK
[4]Department of Physiology, University of Kiel, 24118 Kiel, Germany

The TREK subfamily of two-pore domain (K2P) K^+ channels exhibit polymodal gating by a wide range of physical and chemical stimuli. Crystal structures now exist for these channels in two main states referred to as the "up" and "down" conformations. However, recent studies have resulted in contradictory and mutually exclusive conclusions about the functional (i.e., conductive) status of these two conformations. To address this problem, we have used the state-dependent TREK-2 inhibitor norfluoxetine that can only bind to the down state, thereby allowing us to distinguish between these two conformations when activated by different stimuli. Our results reconcile these previously contradictory gating models by demonstrating that activation by pressure, temperature, voltage, and pH produce more than one structurally distinct open state and reveal that channel activation does not simply involve switching between the up and down conformations. These results also highlight the diversity of structural mechanisms that K2P channels use to integrate polymodal gating signals.

The Journal of General Physiology

INTRODUCTION

The TREK subfamily of two-pore domain potassium (K2P) channels (TREK-1/K2P2.1, TREK-2/K2P10.1, and TRAAK/K2P4.1) exhibit regulation by a diverse array of chemical and physical stimuli. This polymodal regulation serves to couple changes in cellular electrical activity to many different cellular and environmental signals (Enyedi and Czirják, 2010; Renigunta et al., 2015; Sepúlveda et al., 2015). These channels are expressed extensively in the central and peripheral nervous system where their sensitivity to changes in temperature and touch is thought to play an important role in the perception of pain. For example, TREK-2 is found in primary afferent neurons in the dorsal root ganglion (DRG) where it is involved in determining the resting membrane potential and excitability of these cells (Kang and Kim, 2006; Acosta et al., 2014). Also, whole animal experiments have identified a specific role for TREK-2 in both cold and warm thermosensation and in nociception (Pereira et al., 2014).

Extensive functional studies demonstrate that TREK-2 channel activity can be regulated by changes in intracellular (pH_i) and extracellular pH (pH_{ext}), membrane stretch, voltage, temperature, lipids and polyunsaturated fatty acids, various GPCR-coupled signaling pathways, and a wide range of clinically relevant drugs (Kim et al., 2001b; Renigunta et al., 2015). Similar regulatory mechanisms also appear to control the activity of the related TREK-1 and TRAAK channels (Kim et al., 2001a) and provide a clear method for linking channel activity to their proposed physiological roles. However, the structural mechanisms that couple these different stimuli to channel gating remain poorly understood.

Unlike many other K^+ channels, TREK channels do not appear to have a classical helix bundle-crossing gate and instead appear to gate primarily within the selectivity filter (Zilberberg et al., 2001; Piechotta et al., 2011; Rapedius et al., 2012). Together with other studies, this produced an early gating model where movement of the transmembrane (TM) helices allowed coupling of the C-terminal regulatory domain (CTD) and certain regulatory signals to the filter gating mechanism but did not involve closure of a lower helix bundle-crossing gate (Bagriantsev et al., 2011, 2012; Piechotta et al., 2011; Rapedius et al., 2012; Renigunta et al., 2015).

Subsequent crystal structures of the TRAAK channel with the TM helices in different orientations began to provide some structural insight into these processes by revealing two main conformational states of the channel both lacking a bundle-crossing gate. In the "down" state, a gap between the TM helices exposes side portals or fenestrations, whereas in the "up" conformation, an upward movement of the helices, in particular TM4, closes these side fenestrations. However, these studies came to

Correspondence to Stephen J. Tucker: stephen.tucker@physics.ox.ac.uk

Abbreviations used in this paper: CTD, C-terminal regulatory domain; NFx, norfluoxetine; pH_{ext}, extracellular pH; pH_i, intracellular pH; TM, transmembrane.

The Rockefeller University Press $30.00
J. Gen. Physiol. 2016 Vol. 147 No. 6 497–505
www.jgp.org/cgi/doi/10.1085/jgp.201611601

markedly opposite and mutually exclusive conclusions about the functional (i.e., conductive) status of these different conformational states (Brohawn et al., 2012, 2013, 2014; Lolicato et al., 2014); one study proposed that the down conformation of TRAAK represents the closed state and activation requires movement from the down to up state (Brohawn et al., 2014), whereas the other study proposed that activation involves stabilization of the down state and movement from the up to the down state (Lolicato et al., 2014).

In a parallel study, we solved structures of the human TREK-2 channel in two distinct conformations similar to those identified for TRAAK, i.e., up and down conformations. In the same study, we also determined a structure of TREK-2 in complex with two state-dependent inhibitors, fluoxetine and its active metabolite norfluoxetine (NFx; Dong et al., 2015). These structures provided a valuable insight into the functional relevance of the up and down conformations because both drugs have previously been shown to regulate TREK channel activity in a state-dependent manner via the closed state (Kennard et al., 2005). Importantly, our crystal structures identified the binding site for these two inhibitors within the side fenestrations of the channel, binding sites that are only available in the down state as the result of closure of the fenestrations in the up state (Dong et al., 2015). We were also able to demonstrate that membrane stretch produces a large reduction in NFx inhibition, thereby supporting a model for mechanical activation of TREK-2 that involves movement from the down to the up state (Dong et al., 2015). This is illustrated by the cartoon in Fig. 1 A.

Initially, a binary two-state, down to up model for activation of TREK-2 appeared consistent with the conformational changes proposed for stretch activation of TRAAK (Brohawn et al., 2014), but it did not explain why other mechanisms of activation such as intracellular acidification do not produce similar conformational changes (Dong et al., 2015), nor was it consistent with the model that proposes the down conformation as the activated state (Lolicato et al., 2014). We therefore hypothesized that because K2P channel gating occurs primarily within the selectivity filter, then this gate may be able to open independently in both the down and the up states (Dong et al., 2015). Consequently, not all stimuli, in particular those that regulate the filter gate directly (Zilberberg et al., 2001; Sandoz et al., 2009; Bagriantsev et al., 2012; Schewe et al., 2016), may induce the same conformational changes in the TM helices.

In this study, we have taken advantage of our recent structural understanding of the state-dependent inhibition of TREK-2 by NFx to probe the conformational changes that occur in response to activation by a wide range of physiologically relevant stimuli. Our results demonstrate that TREK-2 can interconvert between structurally distinct open conformations when activated by different environmental and chemical stimuli. This provides a structural insight into how polymodal TREK channels use structurally diverse gating mechanisms to integrate a wide range of stimuli into changes in electrical signaling. Furthermore, the results propose a gating model that now accommodates several previously conflicting models.

MATERIALS AND METHODS

Molecular biology and oocyte expression

Oocytes were prepared for injection of mRNA by collagenase digestion followed by manual defolliculation and stored in ND96 solution, which contained (mM) 96 NaCl, 2 KCl, 1.8 $CaCl_2$, 1 $MgCl_2$, and 10 HEPES, pH 7.4, and was supplemented with 2.5 mM sodium pyruvate, 50 µg/ml gentamycin, 50 µg/ml tetracycline, 50 µg/ml ciprofloxacin, and 100 µg/ml amikacin. Full-length human TREK-2 isoform 3 (NCBI Protein database accession no. NP_612191) was used throughout this study and was subcloned into the pBF vector for expression in oocytes. The truncated temperature-insensitive mutant (TREK-2ΔN/ΔC; Dong et al., 2015) contains a deletion of 71 residues at the N terminus and 213 residues at the C terminus. Cells were injected with 1–4 ng mRNA up to 4 d after isolation. In vitro transcription of mRNA was performed using the AmpliCap SP6 kit (Cambio). Experiments were performed 12–24 h after injection at room temperature (22°C unless otherwise indicated). For measurement and comparison of basal whole-cell currents, oocytes were injected with 4 ng RNA and recorded exactly 24 h after injection.

Electrophysiology and data analysis

Patch clamp. Giant-patch electrodes were pulled from thick-walled borosilicate glass and polished to give pipette resistances around 0.4–0.8 MΩ when filled with patch solution. Pipette solution contained (mM) 116 NaCl, 4 KCl, 1 $MgCl_2$, 1.8 $CaCl_2$, and 10 HEPES, pH 7.4, whereas bath solution contained (mM) 120 KCl, 1 NaCl, 2 EGTA, and 10 HEPES, pH 7.3. Patches were perfused via a gravity flow perfusion system. Data were acquired with pCLAMP and recorded using an Axopatch 200B (Molecular Devices), filtered at 1 kHz and sampled at 10 kHz. Macroscopic currents from inside-out patches were recorded from voltage ramps and steps as described for each experiment (see figure legends). For Rb^+ activation, the KCl in the bath solution was replaced by RbCl. As recordings from TREK channels have a propensity to run up in excised patch clamp experiments, only patches where currents stabilized within 1 min after excision were used for analysis. For quantification of stretch activation, only patches with basal currents >150 pA (at 60 mV) were used. Currents from 0-mV steps were reported unless stated otherwise. NFx (Toronto Research Chemicals) was dissolved in DMSO and

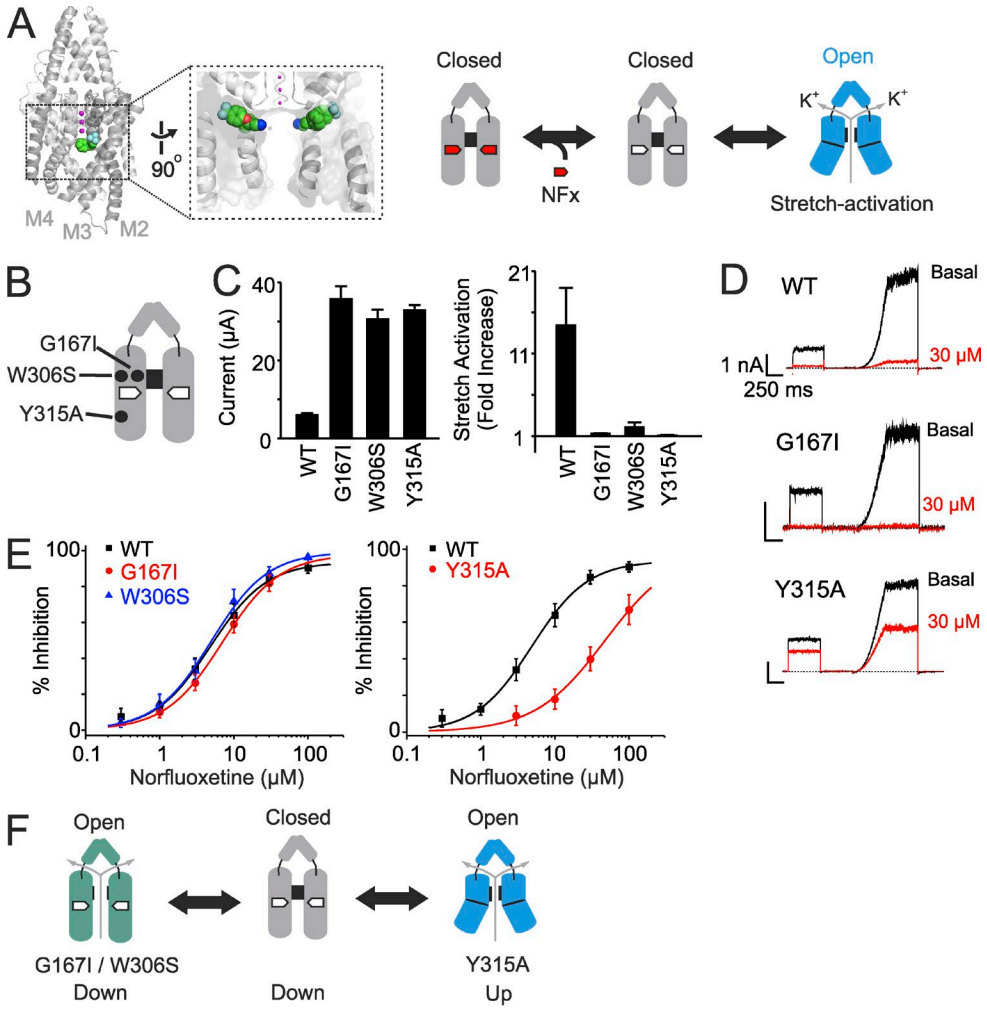

Figure 1. **The down state can be conductive.** (A, left) Structure of TREK-2 in the down state showing NFx (as colored spheres) bound within the fenestrations (Dong et al., 2015). K^+ ions within the filter are shown in magenta. (right) Cartoon model illustrating how activation by membrane stretch reduces inhibition by NFx (red pentagon). In the unbound down state (middle), the filter gate is closed. The NFx-binding site is only found in the down state; thus, channel activation by membrane stretch (up state, blue) reduces availability of the NFx-binding site. This binary two-state model of gating assumes the down state is always closed and the up state is always open. (B) Relative position of the filter gate mutations (G167I and W306S) that directly activate TREK-2 and the Y315A mutation in TM4, which affects movement between the down and up states. (C) All three mutations produce similar increases in basal whole-cell currents recorded at 100 mV ($n \geq 20$; left) and similar reductions in fold activation by membrane stretch (right); currents were recorded in inside-out patches at 0 mV before and after application of negative pressure. Error bars shown are mean ± SEM ($n = 5$). (D) Example traces showing inhibition by 30 μM NFx inhibition for WT and mutant channels. The voltage protocol involves a step to 0 mV from a holding potential of −80 mV, followed by a ramp from −100 to 60 mV. (E) Dose–response curves showing NFx inhibition is unaffected by the filter gate mutations (G167I and W306S) but reduced by the Y315A mutation. WT IC_{50} 4.9 ± 0.5 μM, $n = 16$ compared with G167I (IC_{50} 7.0 ± 0.6 μM, $n = 10$), W306S (IC_{50} 5.0 ± 0.4 μM, $n = 10$), and Y315A (IC_{50} > 30 μM, $n = 8$). Error bars shown are mean ± SEM ($n \geq 6$). (F) Revised gating model showing that channels activated by the filter gate mutations are in the down state, whereas activation by the Y315A mutation affects movement between states to reduce NFx inhibition.

diluted to working concentrations on the day of experimenting (max final DMSO concentration was 0.3%). Percentage inhibition was calculated from stable basal currents after excision using the equation below:

$$\%\ \text{inhibition} = \left(1 - \left(\frac{I_{inh}}{I_{basal}}\right)\right) \cdot 100,$$

where I_{inh} refers to the recorded current in each concentration of NFx and I_{basal} refers to the measured current before drug administration. For tests of mechanosensitivity, 11 mmHg of negative pressure was applied through the patch pipette manually using a 1-ml syringe (calibrated using a Druic DPI260 pressure indicator). Fold activation was calculated from the following equation:

$$\text{Fold activation} = \frac{I_{activated}}{I_{basal}},$$

where $I_{activated}$ refers to the current level after application of activating stimuli and I_{basal} refers to the stable

basal current. Data are presented as mean ± SEM. Dose–response curves were fitted using the Hill equation below:

$$\%\ \text{inhibition} = Iinh_{max} \cdot \left(\frac{[\text{drug}]^H}{IC_{50}{}^H + [\text{drug}]^H}\right),$$

where $Iinh_{max}$ represents the maximal inhibition, [drug] the concentration of inhibitor, IC_{50} the concentration eliciting 50% of the maximal effect, and H the Hill coefficient.

Whole-cell currents. For two-electrode voltage-clamp recordings, electrodes were pulled from thick-walled borosilicate glass and filled with 3 M KCl. ND96 bath solution was used for all recordings; pH was adjusted using either NaOH or HCl and controlled for temperature. Oocytes were perfused with solution via a peristaltic pump perfusion system. Data were acquired with pCLAMP and recorded using a GeneClamp 500 amplifier (Molecular Devices). Whole-cell currents were recorded from voltage protocols as described for each experiment (see figure legends). Temperature was controlled via an in-line perfusion heating controller (Multi Channel Systems).

RESULTS

Mutations activate TREK-2 via structurally distinct mechanisms

One of the two conflicting models for TRAAK channel activation is based on crystal structures of gain-of-function mutations (G124I and W262S) found to be in the down state. This led to the hypothesis that channel activation stabilizes the down state of the channel (Lolicato et al., 2014). These two activatory mutations were originally identified in the related TREK-1 channel by complementation of a K^+ uptake–deficient strain of yeast (Bagriantsev et al., 2011). They are located close to the selectivity filter and were shown to increase channel activity through an increase in open probability. We therefore introduced equivalent mutations in TREK-2 (Fig. 1 B) and expressed them in *Xenopus laevis* oocytes. We found that both the G167I mutation in the first pore helix and the W306S mutation in TM4 markedly increased basal whole-cell currents compared with WT TREK-2 (Fig. 1 C). Both mutants also showed significantly reduced stretch activation when measured using inside-out patches from oocytes expressing these channels (Fig. 1 C). Therefore, similar to their effect on TREK-1 and TRAAK, these two mutants also appear to activate TREK-2, probably via an increase in open probability, which then reduces further activation by membrane stretch.

Based on the model shown in Fig. 1 A, if these two mutants also activate the channel via the same structural mechanism as membrane stretch (i.e., by inducing movement toward the up conformation and closure of the fenestrations) and NFx inhibits channel activity via interaction with its binding site in the fenestration (Dong et al., 2015), then channel inhibition by NFx should be reduced in these mutants. However, we found that NFx inhibition of these two mutants was unaffected in excised inside-out patches (Fig. 1, D and E). This indicates that the NFx-binding site within the fenestrations of the TM helices in these activated channels must still be accessible, and the channels cannot be in the up conformation where the NFx-binding site does not exist.

We have also previously shown that the Y315A mutation activates TREK-2 and leads to a blunted response to stretch activation (Fig. 1 C; Dong et al., 2015). However, unlike G124I and W262S, the Y315A mutation produced a marked reduction in NFx sensitivity (Fig. 1, D and E), suggesting that it affects the conformation of the TM helices. This is consistent with the location of this residue in the middle of the TM4 helix in a region that undergoes a large structural rearrangement when the channel moves between the up and down conformations (Dong et al., 2015). Together, these results suggest that not all activatory mutations operate via the same structural mechanisms and that the G167I and W306S mutations directly activate the filter gate without closure of the fenestration (Fig. 1 F).

Dynamic structural changes in response to channel activation

We have previously reported that membrane stretch reduces NFx inhibition (Dong et al., 2015), and we now show that these dramatic shifts in NFx sensitivity can occur dynamically within the same channels, i.e., before and after stretch activation in the same membrane patch (Fig. 2 A). Similar dynamic changes can also be observed in channels first activated by pH_i and then by membrane stretch (Fig. 2, B and C). This demonstrates that these different functional states of the channel are represented by structurally distinct open conformations capable of interconversion.

To further examine whether these different conformations can be observed within the same channel, we next measured the effect of using membrane stretch to induce a conformational change in the G167I mutant. As shown above (Fig. 1, C–E), this activatory mutation leads to large basal currents, and the functional response of this mutant to stretch activation is markedly reduced, yet it retains full inhibition by NFx. To exclude the possibility that repeated application of the NFx results in any apparent reduction in sensitivity for this mutant, we first measured inhibition in response to consecutive doses and found the extent of inhibition undiminished (Fig. 2 D).

We next examined whether membrane stretch could reduce NFx inhibition in the G167I mutant by inducing a conformational change similar to that in the WT channel during stretch activation. We found that, like

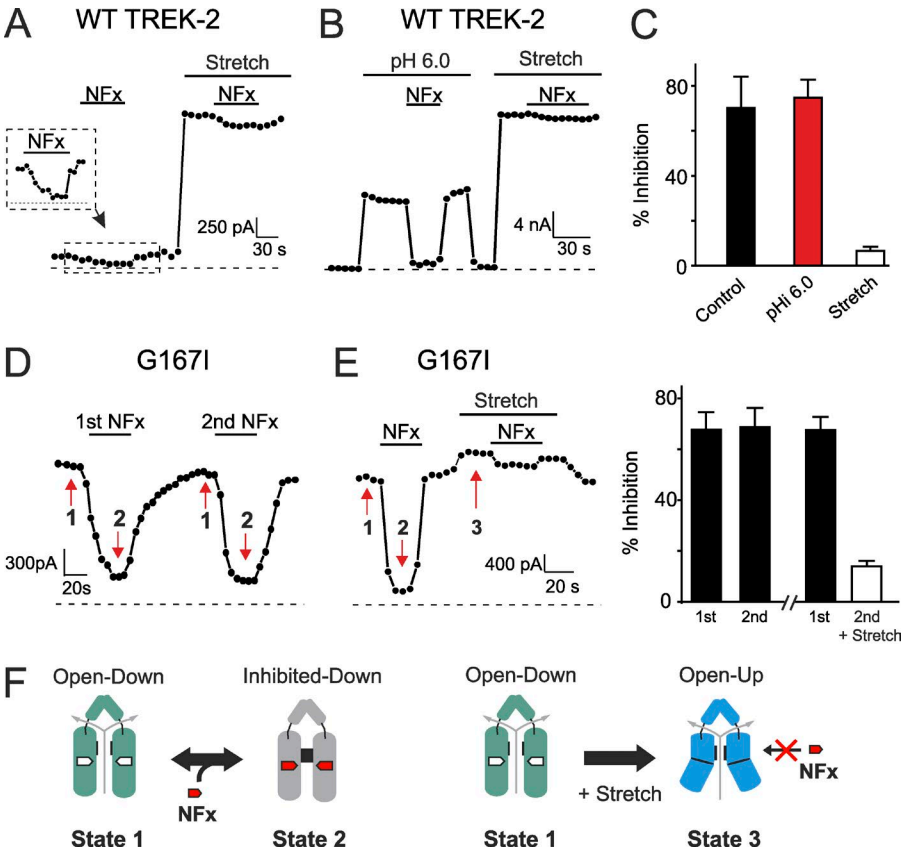

Figure 2. **Dynamic interconversion between structurally distinct open conformations.** (A) Example showing WT TREK-2 currents from an inside-out patch; at pH_i 7.4, channels can be inhibited by 10 µM NFx (effect magnified within inset dashed box). Channels were then stretch activated by application of negative pressure (−11 mmHg suction to the pipette), whereupon NFx inhibition is markedly reduced. Currents were recorded from voltage steps to 0 mV from a holding potential of −80 mV. The dashed line indicates the zero current level. (B) Similar dynamic changes in NFx inhibition can also be observed for channels activated by intracellular acidification (pH_i 6.0), demonstrating that these two activated states are structurally distinct. (C) Summary of dynamic changes in NFx inhibition seen for stretch activation but not pH_i activation. (D) Repeated NFx application produces consistent inhibition of the G167I mutant channel. The red arrows indicate distinct structural states of the channel. (E) Example experiment (similar to that shown in A and B) showing a dynamic change in NFx inhibition for the G167I mutant as the channel is converted from the down state to the up by membrane stretch. (C and E) Error bars shown are mean ± SEM ($n \geq 6$). (F) Cartoon illustrating conversion between different structural states of the channel. The numbers refer to states shown by the red arrows in D. (left) The G167I mutation directly activates the filter gate in the down state, and the NFx-binding site remains available, but when the same channel is subjected to membrane stretch (right), it is converted into the up state, which exhibits reduced NFx sensitivity as the result of closure of the fenestration binding site.

WT TREK-2, this mutant can be inhibited by 10 µM NFx (Fig. 2 E), yet when stretch is applied to the same excised patch, this inhibitory effect disappears. This suggests the mutant channels are initially open in the down conformation but are then shifted to the NFx-insensitive up conformation by membrane stretch. Together, these results demonstrate that TREK-2 can exist in structurally discrete open state conformations and also that the channel can dynamically interconvert between these different states within the same patch as illustrated by the model in Fig. 2 F.

Direct activation of the filter gate by polymodal stimuli

To examine activation of the filter gate more directly, we took advantage of the fact that TREK channel activity can be dramatically increased when Rb^+ is used as the permeant ion (Fig. 3 A; Bockenhauer et al., 2001). This ion-flux gating effect is now known to result from direct activation of the filter gate by permeant Rb^+ ions (Schewe et al., 2016). We therefore examined the NFx sensitivity of channels activated by Rb^+ but observed no change in NFx inhibition (Fig. 3 B). This provides strong evidence that direct activation of the filter gate can occur in the absence of major conformational changes that would otherwise disrupt the NFx-binding site.

Changes in pH_{ext} can also modulate whole-cell TREK-2 currents (Fig. 3 C) via direct regulation of a gating mechanism within the filter (Zilberberg et al., 2001; Sandoz et al., 2009; Bagriantsev et al., 2012). We therefore sought to probe the effects of this pH_{ext} gating mechanism on NFx sensitivity. However, altering external pH can profoundly influence the distribution of charged drugs across the cell membrane (Hille, 1977), and so we examined NFx inhibition of mutations that uncouple this pH_{ext}-sensing mechanism from channel gating. Both the H156A and E103Q mutations are known to abolish the sensitivity of TREK-2 to changes in pH_{ext} (Fig. 3 C; Sandoz et al., 2009; Dong et al., 2015). However, we found that the NFx sensitivity of TREK-2 whole-cell currents for these two mutants was unaltered (Fig. 3 D). This suggests that direct modulation of the filter gate by pH_{ext} can also occur without movement of the channel from the down to up conformation.

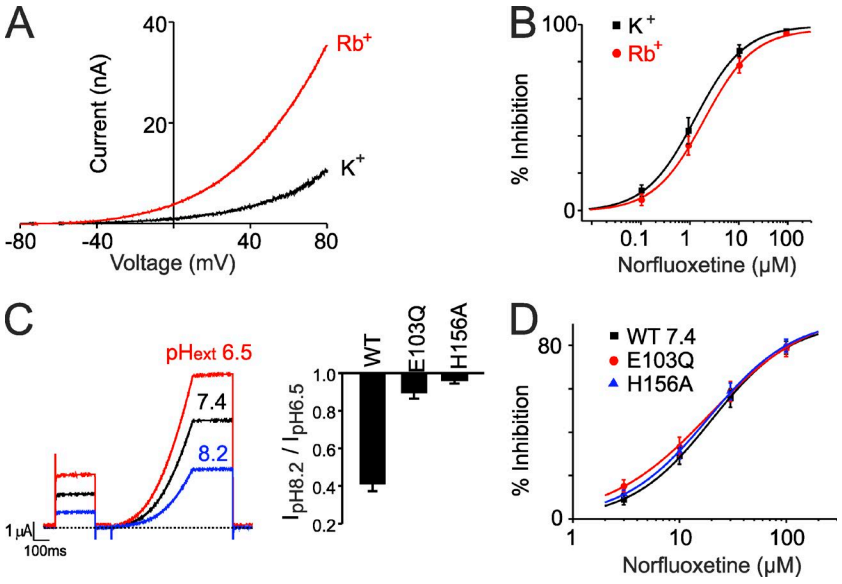

Figure 3. **Direct activation of the filter gate without major conformational changes.** (A) Example traces from inside-out patches showing activation of TREK-2 currents upon exchange of intracellular K^+ for Rb^+. (B) Summary dose–response curves showing NFx inhibition of TREK-2 does not change when Rb^+ is used as the permeant ion to directly activate the filter gate. (C) Example showing activation of whole-cell currents upon extracellular acidification. Bar chart shows the effect of the H156A and E103Q mutations that abolish pH_{ext} activation by interfering with the filter gating mechanism (Dong et al., 2015). (D) Dose–response curves from two-electrode voltage clamp recordings of whole-cell currents showing that neither mutation reduces NFx inhibition (WT IC_{50} = 23.4 ± 3.9 μM, n = 10; E103Q IC_{50} = 18.3 ± 2.3 μM, n = 7; H156A IC_{50} 19.1 ± 2.1 μM, n = 11). Note that when applied extracellularly, higher concentrations of NFx are required to inhibit channel activity. (B–D) Error bars shown are mean ± SEM ($n \geq 6$).

Temperature gating induces a large-scale conformational change of the TM helices

It has also been proposed that temperature activation may induce larger-scale structural changes in the CTD and TM helices, which couple their effects to the filter gate; however, the precise structural mechanisms underlying these activatory mechanisms remain unclear (Kang et al., 2005; Bagriantsev et al., 2012; Schneider et al., 2014). We therefore examined the effect of temperature activation on NFx inhibition.

TREK/TRAAK currents are known to exhibit strong temperature-dependent activation between 22°C and 37°C, but this gating mechanism appears to require cell integrity and is lost upon patch excision (Maingret et al., 2000; Kang et al., 2005). We therefore compared the effect of NFx inhibition on TREK-2 whole-cell currents at different temperatures. Interestingly, we found that temperature activation produces a profound reduction in NFx sensitivity consistent with movement of the TM helices and major conformational changes that would couple the temperature-sensing mechanism to the filter gate (Fig. 4, A and B).

To eliminate any nonspecific effects of this temperature increase, we also examined a truncated form of TREK-2 that retains full sensitivity to NFx inhibition but is no longer temperature sensitive as the result of dele-

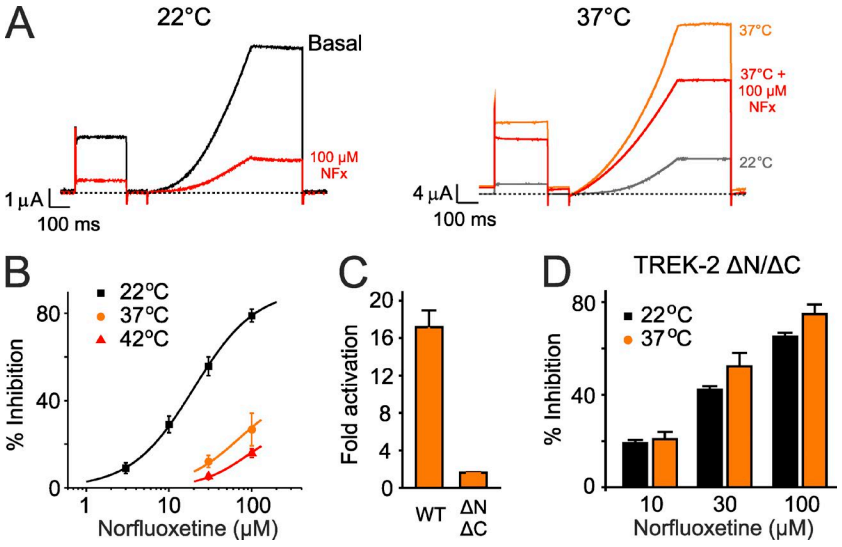

Figure 4. **Temperature activation involves conformational changes in the TM helices.** (A) Example traces showing that temperature-dependent activation of whole-cell TREK-2 currents from 22°C (left) to 37°C (right) markedly decreases inhibition by 100 μM NFx. For comparison, the currents at 22°C are also shown in gray in the right panel. Currents were recorded by voltage protocols similar to those used in Fig. 1 D. (B) Summary dose–response curves showing reduced NFx sensitivity of whole-cell TREK-2 currents at 22°C, 37°C, and 42°C (data shown are percent inhibition of basal currents recorded at 0 mV; mean ± SEM, $n \geq 6$). IC_{50} at 22°C, 23.4 ± 3.1 μM; but at 37°C and 42°C, >100 μM. (C) A truncated version of TREK-2 (TREK2 ΔN/ΔC) that no longer responds to temperature. Fold activation represents change in current between 22°C and 37°C. (D) The NFx sensitivity of this temperature-insensitive mutant is unaffected by temperature, indicating a specific effect on WT TREK-2. (C and D) Error bars shown are mean ± SEM ($n \geq 6$).

tion of the CTD (Fig. 4 C; Kang et al., 2005; Dong et al., 2015). Importantly, the NFx sensitivity of this truncated channel was unaffected by an increase in temperature to 37°C, consistent with a specific temperature-dependent effect on the WT channel (Fig. 4 D).

DISCUSSION

Recent crystal structures of TREK and TRAAK channels in the up and down conformations have resulted in contradictory conclusions about the functional relevance of these structural states. In this study, we have exploited the state-dependent binding of NFx to TREK-2 to examine these different conformational states during activation by a range of polymodal stimuli known to affect channel gating. Our results suggest that TREK-2 can exist in more than one structurally distinct open state and that stimuli that directly activate the filter gate do not necessarily require movement of the channel from the down to the up state. We also show that an activated channel can interconvert between different open states. Importantly, our findings not only help to reconcile two previously conflicting gating models, but also provide insight into the variety of structural mechanisms that control K2P channel gating by polymodal stimuli.

The two conflicting models for TRAAK channel gating both propose a movement between the up and down states during channel gating, but although one study concluded that the up state represents the activated state (Brohawn et al., 2014), the other proposed the down state as the activated state (Lolicato et al., 2014). One of the problems with these binary, two-state gating models is that they assume one conformation to be conductive and the other to be closed. Instead, our data suggest that activation of the filter gate may occur independently in both conformations and that different stimuli influence the probability of opening this gate via distinct structural mechanisms (Fig. 5). Although this gating model is more complex than those suggested for TRAAK, it is not unusual for an ion channel gated by many different stimuli and shares many similarities with the structural gating models proposed for TRP channels, which are also able to act as polymodal signal detectors (Baez-Nieto et al., 2011; Cao et al., 2013).

The basic mechanisms of gating within the TREK/TRAAK channel subfamily are thought to be similar, and so the data supporting our model for TREK-2 gating help reconcile these conflicting models. In particular, the ability of NFx to inhibit channels activated by mutations near the filter (or by permeant ions) clearly demonstrates that these channels must be in a conformation similar to the down state where the binding sites in the fenestrations remain available. Likewise, our data also support the idea that both stretch and temperature activation involve larger-scale conformational changes

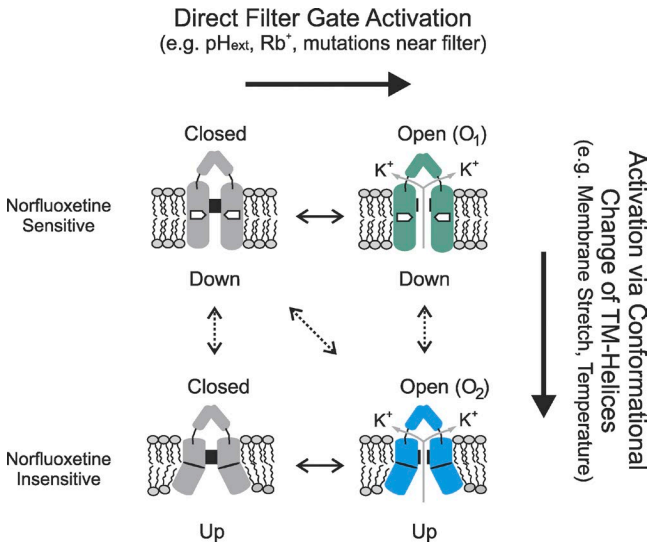

Figure 5. **Expanded gating model for TREK-2 activation.** This cartoon illustrates how structurally distinct open states (e.g., O_1 and O_2) can be produced by different activatory stimuli. The model allows for the filter to gate independently in both the up and down conformations. The dotted line illustrates how the major conformational changes in the TM helices caused by, e.g., membrane stretch and temperature can also influence the filter gating mechanism. The model also shows how the channel can interconvert between different open states in response to membrane stretch.

of the TM helices that converge on a common gate within the filter (Bagriantsev et al., 2011, 2012).

Despite these similarities, our model for TREK-2 mechanosensitivity differs from that proposed for TRAAK in the mechanism responsible for opening the conduction pathway. For TRAAK, it has been proposed that lipids block the inner pore in the down state but not the up state (Brohawn et al., 2014). However, this lipid occlusion model does not easily account for the ability of TREK-2 to be activated in the absence of membrane stretch. Instead, our model suggests that the conformational changes induced by membrane stretch directly activate the filter gate. Our observation that temperature appears to produce similar conformational changes in the TM helices also supports previous models for temperature activation of TREK channels (Bagriantsev et al., 2012) and is consistent with predictions about the structural changes that may underlie the temperature sensitivity of TRP channels (Clapham and Miller, 2011). Importantly, this result also highlights the fact that the functional effect of fluoxetine (Prozac) on K2P channels may be very different in vivo, i.e., at 37°C compared with room temperature (22°C) where experimental data are often collected.

Our results also provide insight into how some stimuli appear to directly activate the filter gate without inducing major conformational changes. However, these more direct mechanisms may also involve other more subtle

structural changes that do not alter the fenestration binding sites for NFx. For example, pH_i activation is thought to require structural changes in the proximal CTD (Honoré et al., 2002), yet pH_i-activated channels retain NFx sensitivity (Fig. 2, B and C; Dong et al., 2015), and so any associated movement of TM helices must be limited in comparison with those changes induced by membrane stretch. Furthermore, a synergistic relationship between pH_i and mechanoactivation has also been demonstrated (Maingret et al., 1999; Kim et al., 2001a,b), and our model suggests how these distinct regulatory pathways might be interactive. For example, the reported increase in mechanosensitivity of channels already activated by pH_i might result from a lower energetic barrier for accessing the stretch-activated state from the pH-activated state than from the closed state (Fig. 5).

Nevertheless, the precise mechanisms that gate the filter open remain unclear. Crystal structures of TREK-2 in the up and down states reveal differences in ion occupancy in the selectivity filter (Dong et al., 2015), but fewer differences are seen in the equivalent structures of TRAAK (Brohawn et al., 2014; Lolicato et al., 2014). However, the precise mechanisms of filter gating in even well-characterized K^+ channels such as KcsA still remain controversial (Liu et al., 2015), and it may not be possible to draw detailed conclusions from the limited range of K2P structures currently available. Even so, our results suggest that certain polymodal stimuli such as pressure and temperature are allosterically coupled to this filter gating mechanism via structural rearrangements of the TM helices, whereas other mechanisms such as changes in pH_{ext} or the permeant ion (Rb^+) activate the channels via a more direct interaction with the filter gate.

In summary, we now propose a model for polymodal gating of TREK-2 that includes multiple, structurally distinct open conformations. Importantly, this expanded model not only helps reconcile several previously conflicting models, but also now provides a framework for understanding the diversity of structural mechanisms that underlie their regulation by polymodal stimuli.

ACKNOWLEDGMENTS

We thank members of the Tucker, Carpenter, and Baukrowitz laboratories, as well as Keith Buckler and Alistair Mathie for helpful discussions.

This work was supported by a Biotechnology and Biological Sciences Research Council (BBSRC) Industrial Partnership Award and by the Wellcome Trust. T. Baukrowitz was supported by the Deutsche Forschungsgemeinschaft (DFG).

The authors declare no competing financial interests.

Kenton J. Swartz served as editor.

Submitted: 4 April 2016
Accepted: 9 May 2016

REFERENCES

Acosta, C., L. Djouhri, R. Watkins, C. Berry, K. Bromage, and S.N. Lawson. 2014. TREK2 expressed selectively in IB4-binding C-fiber nociceptors hyperpolarizes their membrane potentials and limits spontaneous pain. *J. Neurosci.* 34:1494–1509. http://dx.doi.org/10.1523/JNEUROSCI.4528-13.2014

Baez-Nieto, D., J.P. Castillo, C. Dragicevic, O. Alvarez, and R. Latorre. 2011. Thermo-TRP channels: biophysics of polymodal receptors. *Adv. Exp. Med. Biol.* 704:469–490. http://dx.doi.org/10.1007/978-94-007-0265-3_26

Bagriantsev, S.N., R. Peyronnet, K.A. Clark, E. Honoré, and D.L. Minor Jr. 2011. Multiple modalities converge on a common gate to control K2P channel function. *EMBO J.* 30:3594–3606. http://dx.doi.org/10.1038/emboj.2011.230

Bagriantsev, S.N., K.A. Clark, and D.L. Minor Jr. 2012. Metabolic and thermal stimuli control $K_{2P}2.1$ (TREK-1) through modular sensory and gating domains. *EMBO J.* 31:3297–3308. http://dx.doi.org/10.1038/emboj.2012.171

Bockenhauer, D., N. Zilberberg, and S.A. Goldstein. 2001. KCNK2: reversible conversion of a hippocampal potassium leak into a voltage-dependent channel. *Nat. Neurosci.* 4:486–491. http://dx.doi.org/10.1038/87434

Brohawn, S.G., J. del Mármol, and R. MacKinnon. 2012. Crystal structure of the human K2P TRAAK, a lipid- and mechano-sensitive K^+ ion channel. *Science.* 335:436–441. http://dx.doi.org/10.1126/science.1213808

Brohawn, S.G., E.B. Campbell, and R. MacKinnon. 2013. Domain-swapped chain connectivity and gated membrane access in a Fab-mediated crystal of the human TRAAK K^+ channel. *Proc. Natl. Acad. Sci. USA.* 110:2129–2134. http://dx.doi.org/10.1073/pnas.1218950110

Brohawn, S.G., E.B. Campbell, and R. MacKinnon. 2014. Physical mechanism for gating and mechanosensitivity of the human TRAAK K^+ channel. *Nature.* 516:126–130. http://dx.doi.org/10.1038/nature14013

Cao, E., M. Liao, Y. Cheng, and D. Julius. 2013. TRPV1 structures in distinct conformations reveal activation mechanisms. *Nature.* 504:113–118. http://dx.doi.org/10.1038/nature12823

Clapham, D.E., and C. Miller. 2011. A thermodynamic framework for understanding temperature sensing by transient receptor potential (TRP) channels. *Proc. Natl. Acad. Sci. USA.* 108:19492–19497. http://dx.doi.org/10.1073/pnas.1117485108

Dong, Y.Y., A.C. Pike, A. Mackenzie, C. McClenaghan, P. Aryal, L. Dong, A. Quigley, M. Grieben, S. Goubin, S. Mukhopadhyay, et al. 2015. K2P channel gating mechanisms revealed by structures of TREK-2 and a complex with Prozac. *Science.* 347:1256–1259. http://dx.doi.org/10.1126/science.1261512

Enyedi, P., and G. Czirják. 2010. Molecular background of leak K^+ currents: two-pore domain potassium channels. *Physiol. Rev.* 90:559–605. http://dx.doi.org/10.1152/physrev.00029.2009

Hille, B. 1977. The pH-dependent rate of action of local anesthetics on the node of Ranvier. *J. Gen. Physiol.* 69:475–496. http://dx.doi.org/10.1085/jgp.69.4.475

Honoré, E., F. Maingret, M. Lazdunski, and A.J. Patel. 2002. An intracellular proton sensor commands lipid- and mechano-gating of the K^+ channel TREK-1. *EMBO J.* 21:2968–2976. http://dx.doi.org/10.1093/emboj/cdf288

Kang, D., and D. Kim. 2006. TREK-2 ($K_{2P}10.1$) and TRESK ($K_{2P}18.1$) are major background K^+ channels in dorsal root ganglion neurons. *Am. J. Physiol. Cell Physiol.* 291:C138–C146. http://dx.doi.org/10.1152/ajpcell.00629.2005

Kang, D., C. Choe, and D. Kim. 2005. Thermosensitivity of the two-pore domain K^+ channels TREK-2 and TRAAK. *J. Physiol.* 564:103–116. http://dx.doi.org/10.1113/jphysiol.2004.081059

Kennard, L.E., J.R. Chumbley, K.M. Ranatunga, S.J. Armstrong, E.L. Veale, and A. Mathie. 2005. Inhibition of the human two-pore domain potassium channel, TREK-1, by fluoxetine and its

metabolite norfluoxetine. *Br. J. Pharmacol.* 144:821–829. http://dx.doi.org/10.1038/sj.bjp.0706068

Kim, Y., H. Bang, C. Gnatenco, and D. Kim. 2001a. Synergistic interaction and the role of C-terminus in the activation of TRAAK K^+ channels by pressure, free fatty acids and alkali. *Pflugers Arch.* 442:64–72. http://dx.doi.org/10.1007/s004240000496

Kim, Y., C. Gnatenco, H. Bang, and D. Kim. 2001b. Localization of TREK-2 K^+ channel domains that regulate channel kinetics and sensitivity to pressure, fatty acids and pHi. *Pflugers Arch.* 442:952–960. http://dx.doi.org/10.1007/s004240100626

Liu, S., P.J. Focke, K. Matulef, X. Bian, P. Moënne-Loccoz, F.I. Valiyaveetil, and S.W. Lockless. 2015. Ion-binding properties of a K^+ channel selectivity filter in different conformations. *Proc. Natl. Acad. Sci. USA.* 112:15096–15100. http://dx.doi.org/10.1073/pnas.1510526112

Lolicato, M., P.M. Riegelhaupt, C. Arrigoni, K.A. Clark, and D.L. Minor Jr. 2014. Transmembrane helix straightening and buckling underlies activation of mechanosensitive and thermosensitive K_{2P} channels. *Neuron.* 84:1198–1212. http://dx.doi.org/10.1016/j.neuron.2014.11.017

Maingret, F., A.J. Patel, F. Lesage, M. Lazdunski, and E. Honoré. 1999. Mechano- or acid stimulation, two interactive modes of activation of the TREK-1 potassium channel. *J. Biol. Chem.* 274:26691–26696. http://dx.doi.org/10.1074/jbc.274.38.26691

Maingret, F., I. Lauritzen, A.J. Patel, C. Heurteaux, R. Reyes, F. Lesage, M. Lazdunski, and E. Honoré. 2000. TREK-1 is a heat-activated background K^+ channel. *EMBO J.* 19:2483–2491. http://dx.doi.org/10.1093/emboj/19.11.2483

Pereira, V., J. Busserolles, M. Christin, M. Devilliers, L. Poupon, W. Legha, A. Alloui, Y. Aissouni, E. Bourinet, F. Lesage, et al. 2014. Role of the TREK2 potassium channel in cold and warm thermosensation and in pain perception. *Pain.* 155:2534–2544. http://dx.doi.org/10.1016/j.pain.2014.09.013

Piechotta, P.L., M. Rapedius, P.J. Stansfeld, M.K. Bollepalli, G. Ehrlich, I. Andres-Enguix, H. Fritzenschaft, N. Decher, M.S. Sansom, S.J. Tucker, and T. Baukrowitz. 2011. The pore structure and gating mechanism of K2P channels. *EMBO J.* 30:3607–3619. (published erratum appears in *EMBO J.* 2011. 30:4515) http://dx.doi.org/10.1038/emboj.2011.268

Rapedius, M., M.R. Schmidt, C. Sharma, P.J. Stansfeld, M.S. Sansom, T. Baukrowitz, and S.J. Tucker. 2012. State-independent intracellular access of quaternary ammonium blockers to the pore of TREK-1. *Channels (Austin).* 6:473–478. http://dx.doi.org/10.4161/chan.22153

Renigunta, V., G. Schlichthörl, and J. Daut. 2015. Much more than a leak: structure and function of K_{2P}-channels. *Pflugers Arch.* 467:867–894. http://dx.doi.org/10.1007/s00424-015-1703-7

Sandoz, G., D. Douguet, F. Chatelain, M. Lazdunski, and F. Lesage. 2009. Extracellular acidification exerts opposite actions on TREK1 and TREK2 potassium channels via a single conserved histidine residue. *Proc. Natl. Acad. Sci. USA.* 106:14628–14633. http://dx.doi.org/10.1073/pnas.0906267106

Schewe, M., E. Nematian-Ardestani, H. Sun, M. Musinszki, S. Cordeiro, G. Bucci, B.L. de Groot, S.J. Tucker, M. Rapedius, and T. Baukrowitz. 2016. A non-canonical voltage-sensing mechanism controls gating in K2P K^+ channels. *Cell.* 164:937–949. http://dx.doi.org/10.1016/j.cell.2016.02.002

Schneider, E.R., E.O. Anderson, E.O. Gracheva, and S.N. Bagriantsev. 2014. Temperature sensitivity of two-pore (K2P) potassium channels. *Curr. Top. Membr.* 74:113–133. http://dx.doi.org/10.1016/B978-0-12-800181-3.00005-1

Sepúlveda, F.V., L. Pablo Cid, J. Teulon, and M.I. Niemeyer. 2015. Molecular aspects of structure, gating, and physiology of pH-sensitive background K_{2P} and Kir K^+-transport channels. *Physiol. Rev.* 95:179–217. http://dx.doi.org/10.1152/physrev.00016.2014

Zilberberg, N., N. Ilan, and S.A. Goldstein. 2001. KCNKØ: opening and closing the 2-P-domain potassium leak channel entails "C-type" gating of the outer pore. *Neuron.* 32:635–648. http://dx.doi.org/10.1016/S0896-6273(01)00503-7